PORTLAND
PRESS

Review Article

Fluorescence fluctuation spectroscopy: an invaluable microscopy tool for uncovering the biophysical rules for navigating the nuclear landscape

David G. Priest[1,2]**, Ashleigh Solano**[1,2]**, Jieqiong Lou**[1,2] **and** ◉ **Elizabeth Hinde**[1,2]

[1]School of Physics, University of Melbourne, Melbourne, Victoria 3010, Australia; [2]Department of Biochemistry and Molecular Biology, Bio21 Institute, University of Melbourne, Melbourne, Victoria 3010, Australia

Correspondence: Elizabeth Hinde (elizabeth.hinde@unimelb.edu.au)

OPEN ○ ACCESS

Nuclear architecture is fundamental to the manner by which molecules traverse the nucleus. The nucleoplasm is a crowded environment where dynamic rearrangements in local chromatin compaction locally redefine the space accessible toward nuclear protein diffusion. Here, we review a suite of methods based on fluorescence fluctuation spectroscopy (FFS) and how they have been employed to interrogate chromatin organization, as well as the impact this structural framework has on nuclear protein target search. From first focusing on a set of studies that apply FFS to an inert fluorescent tracer diffusing inside the nucleus of a living cell, we demonstrate the capacity of this technology to measure the accessibility of the nucleoplasm. Then with a baseline understanding of the exploration volume available to nuclear proteins during target search, we review direct applications of FFS to fluorescently labeled transcription factors (TFs). FFS can detect changes in TF mobility due to DNA binding, as well as the formation of TF complexes via changes in brightness due to oligomerization. Collectively, we find that FFS-based methods can uncover how nuclear proteins in general navigate the nuclear landscape.

Introduction

The genomic DNA of cells from all kingdoms of life is associated with general structuring proteins that package the genome and regulate access of DNA-binding proteins to their specific DNA sequence motifs [1,2]. In every human cell, ∼2 m of DNA is wrapped around histone proteins to form a string of nucleosomes, and the resulting chromatin fibers are compacted into a multilayered three-dimensional chromatin network that fits within a nuclear volume with a diameter of 10 μm [3]. A significant question has been how DNA-binding proteins navigate the crowded nuclear interior and locate their binding sites within this complex chromatin network. Early studies suggested DNA-binding proteins locate their binding sites via a mixture of 3D diffusion and 1D translocation along DNA; so-called 'facilitated diffusion' [4]. However, more recent results showed that while some low abundance proteins in prokaryotes (such as the Lac repressor) may locate their target sites via facilitated diffusion, for higher abundance proteins and in eukaryotic cells, target search is likely dominated by 3D diffusion [5,6].

Diffusing molecules encounter chromatin with differing degrees of local compaction that may influence their diffusive route taken as well as their local concentration in different subnuclear regions due to size exclusion effects. For example, the dynamic rearrangements in nucleosome proximity that transform transcriptionally accessible euchromatin into silenced heterochromatin have been shown to locally redefine the space accessible to nuclear protein diffusion [7–11]. To what extent this chromatin

organization plays an inhibitory or facilitatory role in guiding the diffusive route of nuclear factors to target destinations is not entirely understood. Furthermore, accessing this information with standard live cell imaging has proven to be technically challenging because the rearrangements in chromatin structure that control DNA template access occur on a fast timescale (micro to milliseconds) [7] and are well below the diffraction limit of light [12].

To interrogate the chromatin network organization within an intact nucleus and define the role this structural framework plays in nuclear factor navigation, two perspectives of investigation have emerged. The first approach is to directly study chromatin organization using electron microscopy [12], super-resolution optical microscopy [13–15], histone FRET microscopy [16–19], or techniques based on high throughput identification of DNA sequences that are in spatial proximity to one another in the nucleus [20–24]. The second perspective is to indirectly probe chromatin organization from the point of view of the molecules exploring this complex environment. By this approach, the accessibility of the nuclear landscape toward diffusing molecules is measured using methods such as fluorescence recovery after photobleaching (FRAP) [25–29], single particle tracking (SPT) [30–34] and fluorescence fluctuation spectroscopy (FFS) [35–40] (Figure 1). The application of SPT and FRAP to study nuclear factor dynamics within live cell nuclear architecture has recently been reviewed [41]. Thus here, we focus on methods based on FFS to uncover the biophysical rules for navigating the nuclear space. As outlined in Figure 1, FFS bridges insights derived from SPT with FRAP by detecting nuclear protein mobility at the single molecule level, but with the statistics to draw conclusions on population level events such as nuclear trafficking.

FFS describes a family of analytical methods that when coupled with live cell microscopy and genetically encoded fluorescent tags, can provide a measurement of nuclear protein diffusion, concentration and oligomerization in the context of live cell chromatin organization [35–40]. FFS methods rely on measuring fluctuations
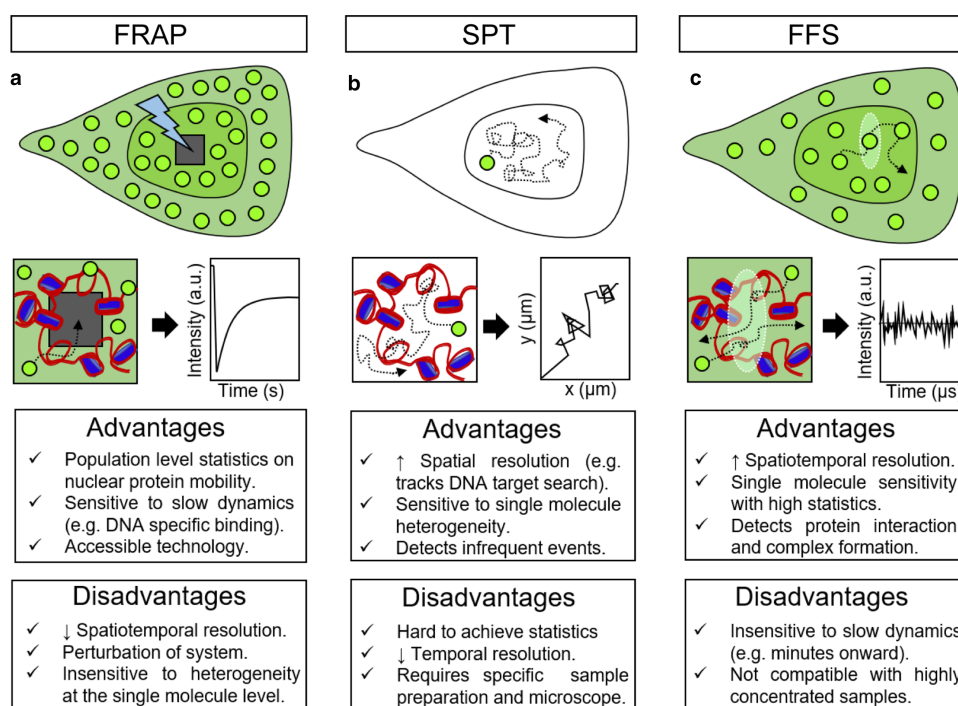
Figure 1. Fluorescence microscopy methods to measure nuclear protein dynamics in a living cell.
(**a**) FRAP. In a nucleus expressing a fluorescently tagged protein, a region of interest (ROI) is photo-bleached and the temporal recovery of fluorescence intensity in this ROI used as a readout of nuclear protein mobility (rate of diffusion). (**b**) SPT. In a nucleus expressing or incubated with a low number of fluorescent molecules, single particles are tracked as a function of time and their trajectories used to calculate mean square displacement and residence times. (**c**) FFS. In a small observation volume (e.g. confocal PSF) parked within a nucleus expressing a low level of fluorescent protein, fluctuations in fluorescence intensity are recorded that have a duration and amplitude indicative of nuclear protein mobility and brightness.

in fluorescence intensity arising from a population of fluorescent molecules passing through a small observation volume [e.g. a confocal or two-photon point spread function (PSF)]. In the case of confocal laser scanning microscopy, the observation volume is either parked in a specific subcellular location of interest (single-point FFS) or scanned across a subcellular compartment (scanning FFS; Figure 2a–c). For every fluorescence fluctuation recorded, two aspects are analyzed. The first is the temporal spectrum, which reports on nuclear protein mobility and can be obtained from a temporal autocorrelation function (ACF) analysis (Figure 2d–g) [42,43]. The second is the amplitude spectrum, which quantifies the number and brightness (NB) (or oligomeric state) of a nuclear protein population and can be obtained from a moment analysis (Figure 2h–k) [44–46] or the generation of a photon counting histogram (PCH) [47]. In the case of scanning FFS, a key advantage is that a spatial component is introduced into the measurement (Figure 2c). Thus, in addition to mapping the local dynamics of a nuclear protein, the diffusive route or law by which it traverses the chromatin environment can be extracted via a spatiotemporal correlation analysis of distinct fluorescence fluctuations.

To demonstrate FFS as an invaluable tool for the study of nuclear architecture and investigate how this structural framework facilitates nuclear protein target search, here we review two types of FFS studies. The first type of study employs an inert fluorescent tracer in a living cell to probe chromatin network microstructure and organization on different temporal and spatial scales [7–11]. This approach provides a spatiotemporal analysis
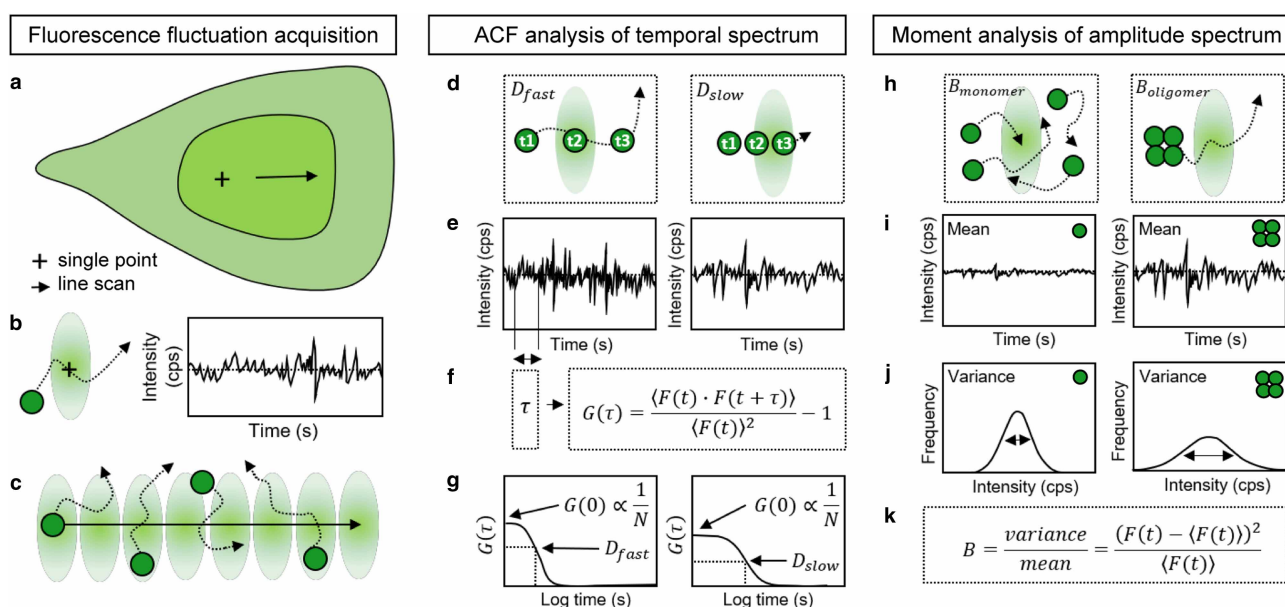
Figure 2. FFS enables protein mobility, concentration and oligomeric state to be quantified in a living cell.
(**a–c**) Schematic of a fluorescence fluctuation acquisition. (**a**) Fluctuations in fluorescence intensity due to protein movement can be acquired in a single point or along a line scan. (**b**) A single-point acquisition (left panel) records fluorescence as a function of time with a microsecond sampling frequency (right panel). (**c**) A line scan acquisition records a series of spatially distinct fluorescence fluctuations with a millisecond sampling frequency. (**d–g**) ACF analysis of the temporal spectrum of a fluorescence fluctuation. (**d**) Schematic of a molecule moving with a fast (D_{fast}) versus slow (D_{slow}) diffusion coefficient through the PSF (observation volume) of a single-point confocal measurement. (**e**) The fluorescence fluctuation that results from the fast versus slow molecule moving through the observation volume. (**f**) The different mobilities within a fluorescence fluctuation ($F(t)$) can be extracted by calculation of the ACF ($G(\tau)$) which essentially correlates a signal with itself for all possible delay times (τ). (**g**) The ACF profile that results has an amplitude at $\tau = 0$ ($G(0)$) that is inversely proportional to the number of molecules (N) at the location of the single-point FFS measurement and a characteristic decay that when fit with a diffusion model can extract the rate of molecular movement (D_{fast} or D_{slow}) through the observation volume. (**h–k**) Moment-based analysis of the amplitude spectrum of a fluorescence fluctuation. (**h**) Schematic of a monomer versus oligomer moving through the PSF of a single-point confocal measurement. (**i**) The fluorescence fluctuation that results from the monomer versus oligomer moving through the observation volume is obviously different despite having a similar mean $\langle F(t) \rangle$ (first moment). (**j**) To quantify the difference between the monomer versus oligomer fluorescence fluctuation depicted in (**i**), the variance must be considered $(F(t)-\langle F(t)\rangle)^2$ (second moment). (**k**) The ratio of the variance (second moment) to the mean (first moment) calculates the brightness of the protein (units, counts per molecule per second).

of the connectivity of the intranuclear landscape, onto which we can overlay a specific nuclear protein's dynamics derived from FRAP-, SPT- or FFS-based experiments. The second type of study is where FFS is applied directly to a biological nuclear protein of interest to track its change in mobility upon interaction with a target site or change in brightness upon complex formation [48–53]. The outcome of this series of studies is a statistical view of how nuclear protein target search is governed by nonspecific versus specific binding interactions and complex formation. This latter point is important since quantifying the impact of oligomer formation on transcription factor (TF) transport dynamics is currently unique to FFS.

Accessibility of the nuclear landscape toward three-dimensional molecular diffusion

Evidence emerging from a series of FFS experiments suggests that modulation of protein access by chromatin is a general mechanism to guide molecules to their correct subnuclear location [7–11]. A key feature of these experiments is to apply FFS to study the mobility of an inert fluorescent tracer (such as free GFP) within a living cell to report on the permeability and therefore microstructure of the intracellular landscape. This approach was first combined with single-point FFS to study the impact of chromatin organization on molecular diffusion [9,11]. For example, in an initial study by Dross et al. [11], the diffusion coefficient of eGFP was derived at several different points inside the nucleus of a living cell and compared with local DNA density (Figure 3a–d). This experiment found that while eGFP mobility varied significantly within the cell nucleus, surprisingly, it did not correlate with chromatin density that was measured via histone H2B tagged to a red fluorescent protein [11]. At the same time, however, in a study by Bancaud et al. [9] the mobility of eGFP oligomers (dimers, pentamers and decamers) was found to be modulated by euchromatin versus heterochromatin. Specifically, the crowded environment of dense heterochromatin reduced the subdiffusive rate of these larger fluorescent tracers two- to three-fold and independently of the number of subunits within the eGFP oligomeric complex [9]. This DNA density-dependent change in mobility has since been observed for monomeric eGFP (albeit to a much subtler extent) when fluorescence fluctuation segments acquired along a scanning FFS experiment are sorted according to local DNA intensity and treated as independent single-point FFS measurements [10]. Collectively, these results suggest that chromatin density, which determines the available volume for molecules to occupy, dictates nuclear protein concentration and mobility. However, given that single-point FFS measures only the local diffusion coefficient of molecules within the PSF (∼0.3 µm), the spatial environment around the PSF and therefore the route the molecules take before crossing the observation volume is not observed. Thus, the diffusive route by which molecules access different subnuclear chromatin environments is not detected.

To investigate the spatial dependence of eGFP mobility within a larger chromatin environment and identify how molecules access different DNA density environments, we mapped the diffusive route of eGFP inside the nucleus of a living cell [7,54,55]. This was achieved by selecting a confocal line scan across regions of high and low DNA density within nuclei of cells stained with Hoechst 33342 (a common chromatin stain). By scanning the laser beam across a selected heterogeneous chromatin environment at a rate faster than eGFP diffusion, fluctuations due to eGFP translocation were recorded and spatiotemporally compared by pair correlation function (pCF) analysis (Figure 3e–h). pCF analysis is a novel approach to spatiotemporal correlation spectroscopy that maps molecular flow along a scanning FFS measurement by calculating the time it takes fluorescent molecules to translocate between pairs of pixels [56]. When applied to free eGFP in a Hoechst-stained nucleus, pCF analysis can detect millisecond changes in local chromatin structure based on the arrival time of eGFP into and out of the chromatin environment [7]. Remarkably, we found that interphase chromatin contains disconnected channels of molecular flow associated with high and low DNA density, but with intermittent bursts of free diffusion between the channels (∼300 ms in duration) that are suggestive of localized fluctuations in chromatin structure. Interestingly, these bursts of 'communication' between the high DNA density channel to the low DNA density environment (where molecular transport is twice as efficient) are dependent on metabolic activity and disappear during mitotic chromosome condensation [54,55]. Collectively, the results from pCF analysis suggest the existence of a not-yet-understood interplay between chromatin organization and molecular flow inside the nucleus.

More recently, Baum et al. employed a related approach, a line-illuminating multi-focus fluorescence microscope, to measure GFP mobility over multiple scales in the nuclei of live cells [8]. This microscopy set-up couples the temporal resolution of single-point FCS (microsecond sampling frequency) with the spatial
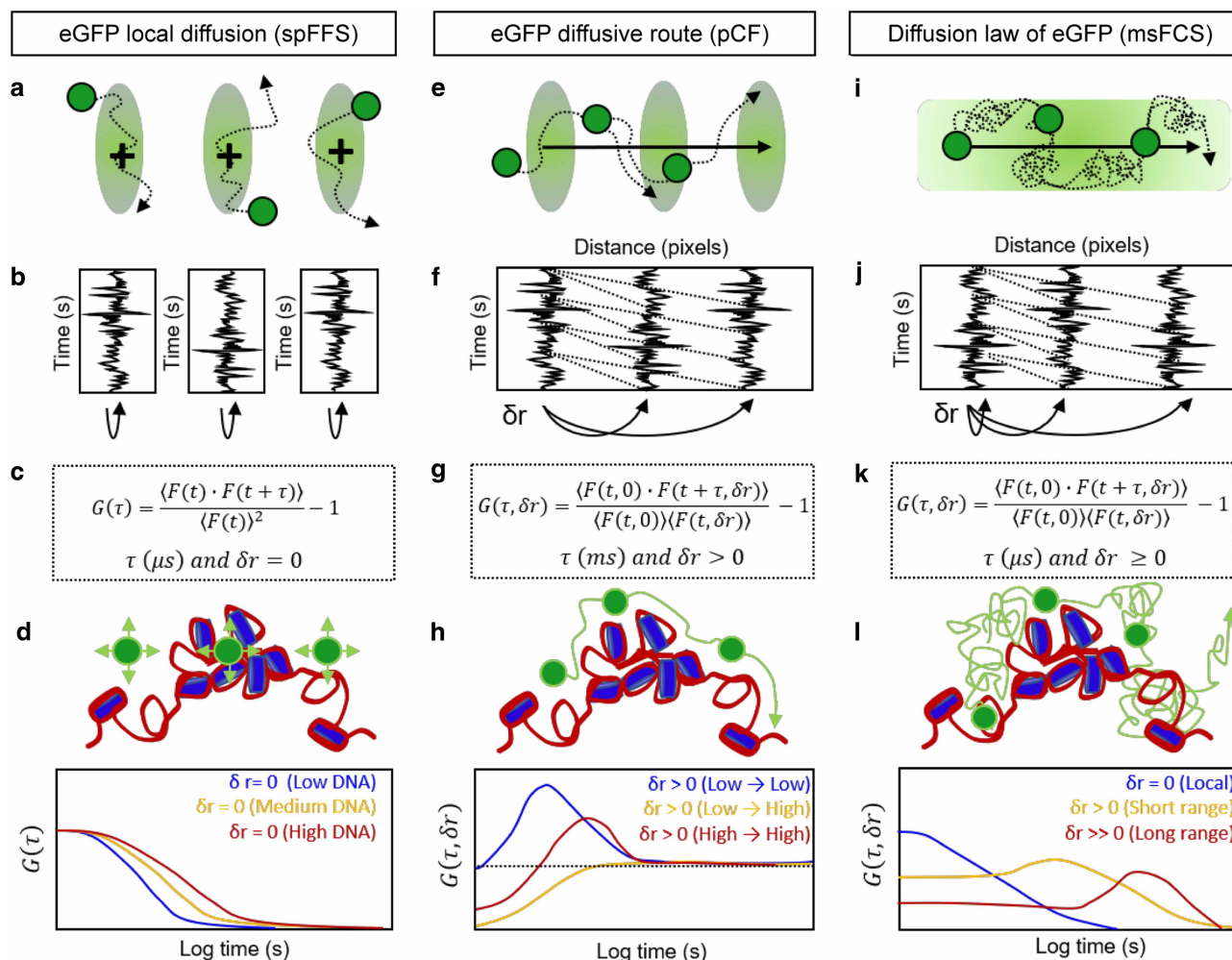
Figure 3. FFS applied to eGFP extracts the accessibility of the nuclear landscape and the biophysical rules for navigating this crowded environment.

(**a–d**) Single-point FFS (spFFS) and ACF analysis of eGFP mobility in the nucleoplasm. (**a**) The mobility of eGFP at different locations within the nucleus can be recovered from the acquisition of a series of spFFS measurements. (**b**) spFFS has a high temporal resolution (microseconds), but single-point measurements do not contain a spatial component. (**c**) eGFP mobility (i.e. the local diffusion coefficient) is extracted from each fluorescence fluctuation ($F(t)$) by application of the ACF ($G(\tau)$) for all possible delay times (τ). (**d**) ACF analysis of spFFS measurements enables correlation of eGFP mobility with local DNA density. (**e–h**) pCF analysis of the diffusive route eGFP adopts along a scanning FFS measurement acquired in the nucleoplasm. (**e**) The diffusive route eGFP adopts inside the nucleus can be tested from the acquisition of a scanning FFS measurement. (**f**) Scanning FFS has a low temporal resolution (milliseconds), but a confocal line scan enables correlation of spatially distinct fluorescence fluctuations. (**g**) The diffusive route of eGFP is extracted by application of the pCF ($G(\tau,\delta r)$) to pairs of fluorescence fluctuations ($F(t)$) separated by a set distance (δr) and for all possible delay times (τ). (**h**) pCF analysis of a scanning FFS measurement enables the diffusive route of eGFP within and between different DNA densities to be quantified. (**i–l**) msFCS applied to a line illuminated FFS measurement acquired in the nucleoplasm. (**i**) The diffusion law by which eGFP traverses the nucleus can be derived from a line illuminated scanning FFS measurement. (**j**) Parallel line illumination offers both high temporal resolution (microseconds) and a spatial component contained within the measurement. (**k**) msFCS involves both application of the ACF ($G(\tau)$) to each fluorescence fluctuation ($F(t)$) and spatial cross correlation ($G(\tau,\delta r)$) of distinct fluorescence fluctuations (analogous to the pCF function). (**l**) A full description of eGFP mobility over multiple length scales ($\delta r \geq 0$) is extracted via msFCS, and this enables the diffusive law by which eGFP explores different chromatin environments to be characterized.

information offered from scanning FCS (sub-micrometer to several micrometers) via the parallelized acquisition of several hundred detection volumes (Figure 3i–l). Thus, a multiscale fluorescence correlation spectroscopy (msFCS) analysis can be performed that extends from an ACF to pCF analysis performed at different distances,

and therefore a mean square displacement analysis of protein transport [8]. Application of this technology to monomeric eGFP confirmed that the nucleus imposes mobility constraints in a scale-dependent manner, and from drug-induced chromatin de-condensation, identified local DNA density as the dominant obstacle restricting certain translocations. Interestingly, comparison of monomeric GFP with multimers of GFP showed that differently sized particles 'sense' distinct structured environments. Larger particles (pentamers) diffuse more slowly and are excluded from certain regions whilst being trapped in other regions, whereas smaller particles (monomers and dimers) diffuse faster and can explore their local environment more thoroughly. This size dependence likely has a significant impact on a nuclear protein's target search mechanism and shifts the threshold for what DNA densities restrict molecular diffusion and access to different nuclear compartments.

FFS-based analysis of TF DNA target search within nuclear architecture

FFS of an inert tracer's mobility inside the nucleus of a living cell has revealed that: (1) local chromatin structure modulates molecular mobility [9–11], (2) global chromatin network organization regulates the diffusive route of nuclear traffic [7,54,55] and (3) the size of the molecule undergoing diffusion influences the exploration volume that can be accessed [8,9]. Deviations from this baseline behavior occur upon binding of a TF to DNA (an immobile obstacle) [8,40,48,52], which is often accompanied by protein–protein interaction and or complex formation (e.g. homo-oligomerization) [35,49–51,53,57]. SPT has proved to be a powerful technique to measure TF diffusion and residence times [41]; however, FFS methods can also access these variables often via simpler experiments. To detect, localize and characterize TF DNA-binding dynamics based on mobility alone, the temporal spectrum of the fluorescence fluctuation is analyzed (Figure 2d–g). In the simplest case, this is performed by an ACF analysis of a single-point FFS measurement that is subsequently fit to a modified diffusion model to account for DNA binding [40,42,43,58].

In an elegant study by Kaur et al. [52] single-point FFS was performed in a developing mouse embryo to investigate the mobility of the TF Oct4 during mammalian development [52]. Oct4 was tagged with photoactivatable GFP (paGFP) to maintain the FFS requirement of a low fluorophore concentration. Then from ACF analysis of Oct4-paGFP movement in single nuclei, it was found that while 75% of Oct4 was freely diffusing, the remaining fraction underwent an anomalous subdiffusive process with a tens of millisecond dwell time. Comparison of the subdiffusive population with free paGFP and an Oct4-paGFP DNA-binding mutant revealed the anomalous component to be a specific property of Oct4 DNA interaction (Figure 4a,b). Furthermore, the anomalous component of Oct4 diffusion was selectively slowed down in the nuclei of pluripotent but not extra-embryonic cells [52]. Given the known role of Oct4 in the maintenance of pluripotency, this set of single-point FFS experiments suggest Oct4 nuclear mobility can accurately predict its functional activity, as confirmed by SPT [59]. TF mobility as a readout of specific DNA binding has since been employed in several different types of scanning FFS-based experiments, with the added advantage of this property being either spatially mapped [e.g. temporal image correlation spectroscopy (tICS)] [40,48,60] or analyzed by a spatiotemporal correlation function that infers mobility over multiple length scales [e.g. multiscale FCS or raster image correlation spectroscopy (RICS)] [8,49]. The aspects of nuclear protein mobility that these different FFS-based methods of analysis can quantify in a living cell are outlined and compared in Table 1.

To investigate if and how TF oligomerization influences DNA target search strategy, given that self-association has long been known to regulate TF function in prokaryotes, the amplitude spectrum of a fluorescence fluctuation provides a valuable additional dimension of information. The amplitude spectrum reports on the brightness of the fluorescent molecules that give rise to a measured fluorescence fluctuation, a property directly related to a fluorescent protein's oligomeric state (Figure 2h–k). In the case of a single-point FFS measurement, where the sampling frequency is fast (microseconds) and good statistics can be achieved, the different brightness species of a TF at a specific location can be extracted by constructing a PCH [47]. PCH analysis, however, requires access to a true photon counting detector. If this hardware is not available, an alternative method to recover the oligomeric state of a TF within a single-point FFS measurement is by moment analysis [44–46]. Moment-based brightness analysis of oligomerization has been applied to several TFs, and in each case, these FFS studies showed that self-association modulates TF DNA-binding activity [35,49–51,53,57]. For example, it was found from tagging the glucocorticoid receptor (GR) with GFP (GFP-GR) that upon binding DNA, GFP-GR dimers form a tetrameric complex that is key to the GR activation pathway (Figure 4c,d).
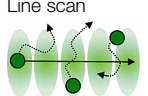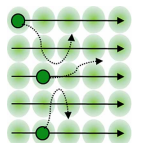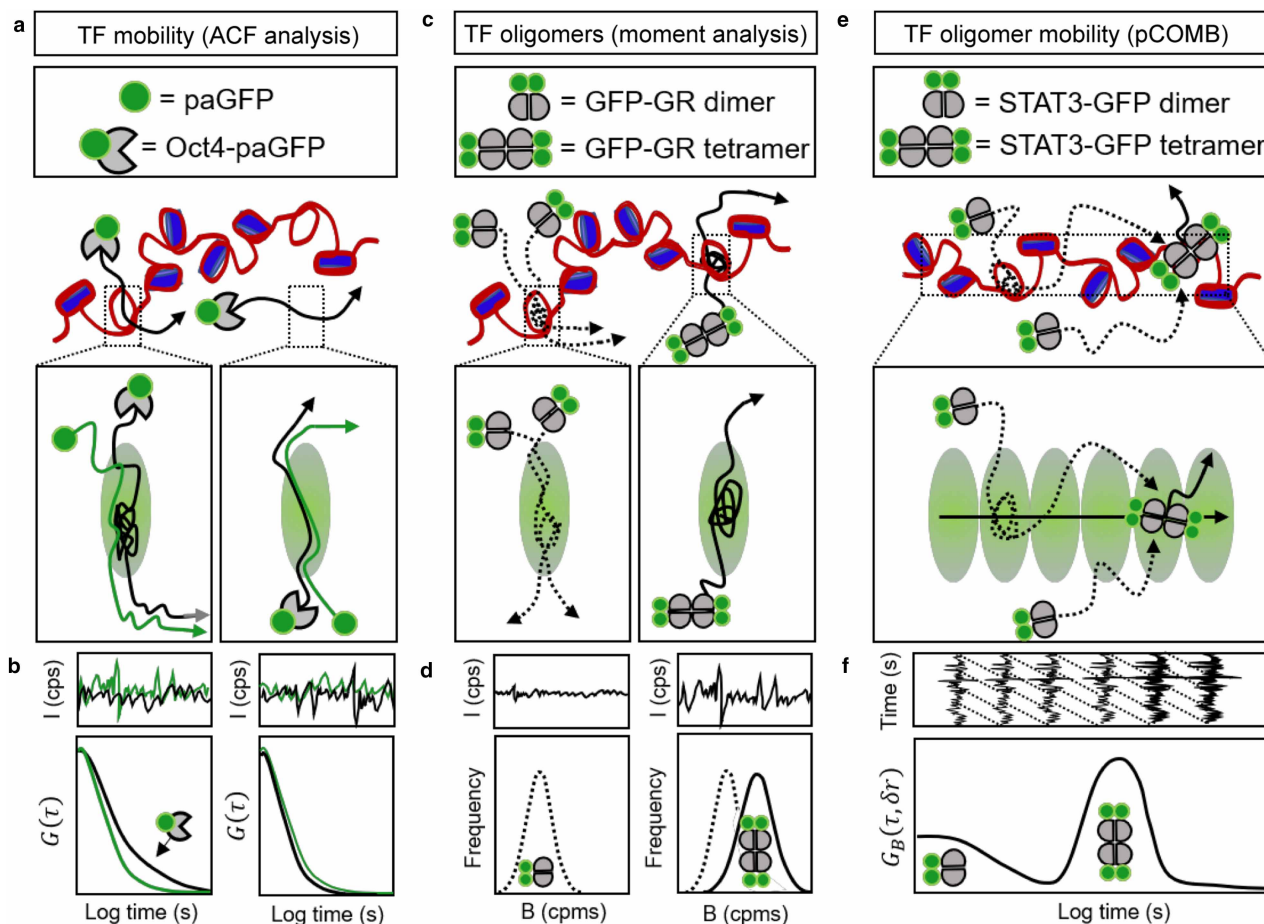
Figure 4. FFS applied to a fluorescently tagged TF enables target search, as well as interaction with the DNA template, to be spatiotemporally tracked.

(**a** and **b**) ACF analysis of TF mobility enables the detection of specific versus non-specific binding to DNA in the nucleus. (**a**) Kaur et al. [52] compare the diffusive behavior of Oct4-paGFP (black trace) with free paGFP (green trace) via the acquisition of FFS measurements and find that the intranuclear mobility of this TF can be used as a readout of Oct4 functional activity (left panel depicts Oct4 interaction with the DNA template). (**b**) ACF analysis of the fluorescence fluctuations that result from Oct4-paGFP movement reveal a 2-component diffusive behavior and the anomalous component was found to be specific to Oct4 DNA binding. (**c** and **d**) Moment-based brightness analysis of TF oligomerization enables detection of complex formation upon DNA binding. (**c**) Presman et al. [53] investigate the role of self-association in GFP-GR transcriptional activity by a moment-based analysis of fluorescence fluctuations. (**d**) The recovered distribution of GFP-GR brightness values reveals DNA binding to trigger GFP-GR dimer assembly into tetramers. (**e** and **f**) pCOMB analysis enables analysis of TF mobility as a function of oligomeric state. (**e**) Hinde et al. [51] develop a method called pCOMB that can track TF oligomer mobility along a scanning FFS measurement and use this technology to investigate STAT3-eGFP DNA target search. (**f**) pCOMB spatiotemporally cross correlates distinct brightness fluctuations to reveal a mobile population of STAT3-eGFP dimers (left peak in bottom plot) which upon binding DNA form and immobilized population of tetramers (right peak).

A critical advantage of moment-based brightness analysis is its applicability to scanning FFS measurements when limited to the first and second moment (i.e. NB analysis) [48,49]. Unlike PCH analysis, which demands high statistics and is computationally too laborious to apply to all pixels within an image, NB analysis enables TF oligomerization to be spatially mapped in the context of live cell nuclear architecture, as has been done with Signal transducer and activator of transcription 3 (STAT3) [51,61]. With this approach, however, the average oligomeric state reported in each pixel can potentially mask the presence of a heterogeneous oligomeric population. Efforts have therefore been made to resolve the different species that can coexist in each pixel of an NB acquisition via the development of time resolved NB and enhanced NB [62,63]. An alternative approach is, however, to filter the different oligomeric species present based on mobility and how this detected oligomeric population evolves in space over time. To do this, we combined the capacity of pCF analysis to track molecular

Table 1 Overview and comparison of FFS methods used to investigate nuclear dynamics

Acquisition	FFS method	Observables of FFS method of analysis	Technical notes of consideration	References
Single point Microsecond sampling	Autocorrelation function (ACF)	- Rate and type of diffusion (2D, 3D, anomalous etc.) - Binding kinetics (association/dissociation rates) - Number of molecules (concentration within point spread function of a single point)	Microsecond sampling frequency enables fast mobilities to be detected (D upto $\sim300 \ \mu m^2 \ s^{-1}$). No spatial component in measurement, thus only local dynamics being analyzed in a single point.	[9,11,36,39, 42–44,52,58]
	Moment-based brightness analysis	- Brightness of a population of molecules - Distribution of aggregation/oligomeric states - Fraction of immobile molecules	First and second moment is sufficient to characterize brightness of a homogenous population. Higher order moments required for a heterogenous population.	[45,46,50, 68–71]
	Photon counting histogram (PCH)	- Stoichiometry of a heterogenous population (number of subunits per complex) in a single point - Fraction of each oligomeric species present	Microsecond sampling frequency enables high statistics, which is a requirement of PCH analysis. This method relies on use of a true photon counting detector.	[47,71,72]
Line scan Microsecond to millisecond sampling + 1D spatial component	Autocorrelation function (ACF)	- Diffusion rate/type, binding kinetics and number of molecules quantified in each pixel along line scan - Option to sort parameters derived in each pixel based on a reference intensity (e.g. DNA density)	Millisecond sampling frequency limits mobilities detected (D upto $\sim30 \ \mu m^2 \ s^{-1}$). Spatial component in measurement enables higher statistics and further detection of heterogeneity in mobility rates and types.	[10,36,73–74]
	Pair correlation function (pCF)	- Quantify the arrival time of a nuclear protein between pairs of points separated by a fixed or varying distance (δr > point spread function) - Detect location and size of barriers to diffusion	Millisecond sampling frequency enables the diffusive route of a nuclear protein population to be mapped over a spatial scale of ~0.3 to $1 \ \mu m$. Pair correlation analysis can also now be applied radially in 2D frame scan acquisitions.	[7,37,54–56, 75–77]
	Multiscale fluorescence correlation spectroscopy (msFCS)	- Diffusion rate/type, binding kinetics (ACF) and arrival time between distinct locations (pCF) - Diffusion law (mean square displacement analysis) - Number of molecules in each pixel along line scan	Microsecond sampling frequency enables fast mobilities to be detected alongside spatial information (e.g. molecular flow and diffusion law). Requires access to a line-illuminating multi-focus fluorescence microscope.	[8]
	Pair correlation of molecular brightness (pCOMB)	- Quantify the mobility of nuclear proteins as a function of oligomeric state and DNA density	Spatial correlation of brightness fluctuations amplifies the presence of few higher order oligomers (perfect for TFs).	[51]
Frame scan Millisecond to second sampling + 2D spatial component	Temporal image correlation spectroscopy (tICS)	- Map nuclear protein mobility as a function of pixel position (favors specific DNA-binding dynamics)	Second sampling frequency limits detection of fast mobilities (i.e. cannot detect free intranuclear diffusion).	[40,48,78–82]
	Raster image correlation spectroscopy (RICS)	- Diffusion rate/type and binding kinetics in a selected ROI with high statistics - Number of molecules in selected ROI	By exploiting the hidden time structure of a confocal raster scan (microsecond, millisecond, second) fast nuclear mobilities can be detected (D upto $\sim300 \ \mu m^2 \ s^{-1}$).	[36,49,83–86]
	Number and brightness (NB)	- Spatially map the number of molecules and their apparent brightness (average oligomeric state) - Option to use enhanced NB which can detect heterogeneous oligomer population in a given pixel	Based on first and second moment analysis. Does not require a true photon counting detector, but if an analogue detector is used, careful calibration of this type of detector is required.	[35,53, 61–63,87–89]
	Spatiotemporal image correlation spectroscopy (STICS)	- Quantify direction and magnitude of molecular flow - Maps of molecular flow velocity	STICS and iMSD both spatially cross correlate images taken at different times. On a confocal system the sampling frequency (seconds) is likely too slow for nuclear protein dynamics and thus access to a light sheet microscope or hilo-TIRF is required for detection of flow/diffusion law.	[90–93]
	Image mean square displacement (iMSD)	- Determine the diffusion law by which proteins move (e.g. isotropic, confined or partitioned)		[94–97]

flow with moment-based detection of oligomerization events [51]. This method, termed pair correlation of molecular brightness (pCOMB), tracks oligomer mobility by first amplifying the signal from the brightest species present and then filtering the dynamics of the extracted oligomeric population based on arrival time between two locations (Figure 4e,f) [51]. Because TF mobility is in general limited upon interaction with the DNA network, pCOMB analysis is sensitive toward changes in oligomeric state that accompany nonspecific or specific DNA binding. Thus, coupled with the knowledge that nuclear protein size modulates exploration of the nucleoplasm, this technology has the potential to provide insight into how TFs employ self-association to navigate nuclear architecture and modulate DNA-binding activity.

Perspectives

- *Importance in the field*: The multilayered 3D arrangement of DNA into the chromatin network renders the nucleoplasm into an incredibly crowded environment and yet nuclear proteins efficiently navigate this structural framework to arrive at a target DNA sequence. How exactly nuclear organization regulates nuclear trafficking to maintain genome function is thus of great interest. As reviewed here, the evidence that has emerged from application of FFS to an inert tracer's mobility inside the nucleus is that modulation of protein access by chromatin constitutes a general mechanism to sequester molecules where they need to be for DNA-dependent activity. Importantly, the detected spatial compartmentalization of the nucleus that is imparted by chromatin is not static and rearranges on a spatiotemporal scale that is only visible when you observe it from the point of view of the molecules scanning the genome [7–11]. Thus, probing nuclear organization from the point of view of the DNA-binding proteins that read and copy genetic information is key.

- *Summary of current thinking*: FFS applied directly to fluorescently labeled TFs enables a unique perspective on DNA target search and how this process is regulated by nuclear architecture. The current thinking derived from FFS analysis of TF mobility is that the biophysical rules which govern inert protein navigation of the nucleoplasm also apply to TF transport, but with DNA-binding interactions of varying affinity overlaid, which result in TF accumulation at specific nuclear locations [48,49,52]. In many instances, the affinity of DNA interaction is increased by homo-oligomerization [50,53,57], and thus the measurement of both TF mobility and brightness (read out of oligomer formation) can serve as a powerful approach to spatiotemporally track TF activity [51].

- *A comment on future directions*: Given the nanoscale nature of the chromatin network [12], in the future it will be essential to develop methods that can probe intranuclear diffusion and TF complex formation at a higher resolution. One way to achieve this is to couple the FFS-based methods of nuclear protein analysis reviewed here (Table 1) with microscopy hardware that reduces the size of the observation volume. Efforts are already underway to do just this via the use of microscope systems with stimulated emission depletion (STED) [64,65] or, more recently, the Zeiss Airyscan detector [66]. These exciting new approaches to the acquisition of FFS data, combined with the use of bright organic dyes that can be linked to the target protein using Halo or SNAP-tags [67], will enable dynamics features such as chromatin accessibility or TF complex formation to be interrogated with unprecedented spatiotemporal resolution. Multiplexing super-resolution with FFS will undoubtedly facilitate our understanding of the interplay between chromatin structure and genome function.

Abbreviations

ACF, autocorrelation function; eGFP, enhanced green fluorescent protein; FCS, fluorescence correlation spectroscopy; FFS, fluorescence fluctuation spectroscopy; FRAP, fluorescence recovery after photobleaching;

GR, glucocorticoid receptor; iMSD, image mean square displacement; msFCS, multi scale fluorescence correlation spectroscopy; NB, number and brightness; pCF, pair correlation function; PCH, photon counting histogram; pCOMB, pair correlation of molecular brightness; PSF, point spread function; RICS, raster image correlation spectroscopy; SPT, single particle tracking; STAT3, Signal transducer and activator of transcription 3; STED, stimulated emission depletion; STICS, spatiotemporal image correlation spectroscopy; TF, transcription factor; tICS, temporal image correlation spectroscopy.

Competing Interests

The authors declare that there are no competing interests associated with the manuscript.

References

1   Dillon, S.C. and Dorman, C.J. (2010) Bacterial nucleoid-associated proteins, nucleoid structure and gene expression. *Nat. Rev. Microbiol.* **8**, 185–195 https://doi.org/10.1038/nrmicro2261
2   Luger, K., Dechassa, M.L. and Tremethick, D.J. (2012) New insights into nucleosome and chromatin structure: an ordered state or a disordered affair? *Nat. Rev. Mol. Cell Biol.* **13**, 436–447 https://doi.org/10.1038/nrm3382
3   Bonev, B. and Cavalli, G. (2016) Organization and function of the 3D genome. *Nat. Rev. Genet.* **17**, 772 https://doi.org/10.1038/nrg.2016.147
4   Mirny, L., Slutsky, M., Wunderlich, Z., Tafvizi, A., Leith, J. and Kosmrlj, A. (2009) How a protein searches for its site on DNA: the mechanism of facilitated diffusion. *J. Phys. A Math. Theor.* **42**, 434013 https://doi.org/10.1088/1751-8113/42/43/434013
5   Redding, S. and Greene, E.C. (2013) How do proteins locate specific targets in DNA? *Chem. Phys. Lett.* **570**, 1–11 https://doi.org/10.1016/j.cplett.2013.03.035
6   Wang, F., Redding, S., Finkelstein, I.J., Gorman, J., Reichman, D.R. and Greene, E.C. (2013) The promoter-search mechanism of *Escherichia coli* RNA polymerase is dominated by three-dimensional diffusion. *Nat. Struct. Mol. Biol.* **20**, 174–181 https://doi.org/10.1038/nsmb.2472
7   Hinde, E., Cardarelli, F., Digman, M.A. and Gratton, E. (2010) In vivo pair correlation analysis of EGFP intranuclear diffusion reveals DNA-dependent molecular flow. *Proc. Natl Acad. Sci. U.S.A.* **107**, 16560–16565 https://doi.org/10.1073/pnas.1006731107
8   Baum, M., Erdel, F., Wachsmuth, M. and Rippe, K. (2014) Retrieving the intracellular topology from multi-scale protein mobility mapping in living cells. *Nat. Commun.* **5**, 4494 https://doi.org/10.1038/ncomms5494
9   Bancaud, A., Huet, S., Daigle, N., Mozziconacci, J., Beaudouin, J. and Ellenberg, J. (2009) Molecular crowding affects diffusion and binding of nuclear proteins in heterochromatin and reveals the fractal organization of chromatin. *EMBO J.* **28**, 3785–3798 https://doi.org/10.1038/emboj.2009.340
10   Di Bona, M., Mancini, M.A., Mazza, D., Vicidomini, G., Diaspro, A. and Lanzanò, L. (2019) Measuring mobility in chromatin by intensity-sorted FCS. *Biophys. J.* **116**, 987–999 https://doi.org/10.1016/j.bpj.2019.02.003
11   Dross, N., Spriet, C., Zwerger, M., Müller, G., Waldeck, W., Langowski, J. et al. (2009) Mapping eGFP oligomer mobility in living cell nuclei. *PLoS ONE* **4**, e5041 https://doi.org/10.1371/journal.pone.0005041
12   Ou, H.D., Phan, S., Deerinck, T.J., Thor, A., Ellisman, M.H. and O'Shea, C.C. (2017) ChromEMT: visualizing 3D chromatin structure and compaction in interphase and mitotic cells. *Science* **357**, eaag0025 https://doi.org/10.1126/science.357.6346.25
13   Schmid, V.J., Cremer, M. and Cremer, T. (2017) Quantitative analyses of the 3D nuclear landscape recorded with super-resolved fluorescence microscopy. *Methods* **123**, 33–46 https://doi.org/10.1016/j.ymeth.2017.03.013
14   Szymborska, A., de Marco, A., Daigle, N., Cordes, V.C., Briggs, J.A.G. and Ellenberg, J. (2013) Nuclear pore scaffold structure analyzed by super-resolution microscopy and particle averaging. *Science* **341**, 655–658 https://doi.org/10.1126/science.1240672
15   Xiang, W., Roberti, M.J., Hériché, J.-K., Huet, S., Alexander, S. and Ellenberg, J. (2018) Correlative live and super-resolution imaging reveals the dynamic structure of replication domains. *J. Cell Biol.* **217**, 1973–1984 https://doi.org/10.1083/jcb.201709074
16   Llères, D., Bailly, A.P., Perrin, A., Norman, D.G., Xirodimas, D.P. and Feil, R. (2017) Quantitative FLIM-FRET microscopy to monitor nanoscale chromatin compaction in vivo reveals structural roles of condensin complexes. *Cell Rep.* **18**, 1791–1803 https://doi.org/10.1016/j.celrep.2017.01.043
17   Llères, D., James, J., Swift, S., Norman, D.G. and Lamond, A.I. (2009) Quantitative analysis of chromatin compaction in living cells using FLIM-FRET. *J. Cell Biol.* **187**, 481–496 https://doi.org/10.1083/jcb.200907029
18   Sherrard, A., Bishop, P., Panagi, M., Villagomez, M.B., Alibhai, D. and Kaidi, A. (2018) Streamlined histone-based fluorescence lifetime imaging microscopy (FLIM) for studying chromatin organisation. *Biol. Open* **7**, bio031476 https://doi.org/10.1242/bio.031476
19   Lou, J., Scipioni, L., Wright, B.K., Bartolec, T.K., Zhang, J., Masamsetti, V.P. et al. (2019) Phasor histone FLIM-FRET microscopy quantifies spatiotemporal rearrangement of chromatin architecture during the DNA damage response. *Proc. Natl Acad. Sci. U.S.A.* **116**, 7323–7332 https://doi.org/10.1073/pnas.1814965116
20   Bickmore, W.A. (2013) The spatial organization of the human genome. *Annu Rev. Genomics Hum. Genet.* **14**, 67–84 https://doi.org/10.1146/annurev-genom-091212-153515
21   Dekker, J. and Mirny, L. (2013) Biological techniques: chromosomes captured one by one. *Nature* **502**, 45–46 https://doi.org/10.1038/nature12691
22   Ohno, M., Ando, T., Priest, D.G., Kumar, V., Yoshida, Y. and Taniguchi, Y. (2019) Sub-nucleosomal genome structure reveals distinct nucleosome folding motifs. *Cell* **176**, 520–534 e525 https://doi.org/10.1016/j.cell.2018.12.014
23   Ohno, M., Priest, D.G. and Taniguchi, Y. (2018) Nucleosome-level 3D organization of the genome. *Biochem. Soc. Trans* **46**, 491–501 https://doi.org/10.1042/BST20170388
24   Quinodoz, S.A., Ollikainen, N., Tabak, B., Palla, A., Schmidt, J.M., Detmar, E. et al. (2018) Higher-order inter-chromosomal hubs shape 3D genome organization in the nucleus. *Cell* **174**, 744–757 e724 https://doi.org/10.1016/j.cell.2018.05.024
25   Erdel, F., Müller-Ott, K., Baum, M., Wachsmuth, M. and Rippe, K. (2011) Dissecting chromatin interactions in living cells from protein mobility maps. *Chromosome Res.* **19**, 99–115 https://doi.org/10.1007/s10577-010-9155-6
26   Erdel, F. and Rippe, K. (2012) Quantifying transient binding of ISWI chromatin remodelers in living cells by pixel-wise photobleaching profile evolution analysis. *Proc. Natl Acad. Sci. US.A.* **109**, E3221–E3230 https://doi.org/10.1073/pnas.1209579109

27 Bancaud, A., Huet, S., Rabut, G. and Ellenberg, J. (2010) Fluorescence perturbation techniques to study mobility and molecular dynamics of proteins in live cells: FRAP, photoactivation, photoconversion, and FLIP. *Cold Spring Harb. Protoc.* **2010**, pdb.top90 https://doi.org/10.1101/pdb.top90

28 McNally, J.G. (2008) Quantitative FRAP in analysis of molecular binding dynamics in vivo. *Methods Cell Biol.* **85**, 329–351 https://doi.org/10.1016/S0091-679X(08)85014-5

29 Stasevich, T.J., Mueller, F., Brown, D.T. and McNally, J.G. (2010) Dissecting the binding mechanism of the linker histone in live cells: an integrated FRAP analysis. *EMBO J.* **29**, 1225–1234 https://doi.org/10.1038/emboj.2010.24

30 Caccianini, L., Normanno, D., Izeddin, I. and Dahan, M. (2015) Single molecule study of non-specific binding kinetics of LacI in mammalian cells. *Faraday Discuss* **184**, 393–400 https://doi.org/10.1039/C5FD00112A

31 Izeddin, I., Récamier, V., Bosanac, L., Cissé, I.I., Boudarene, L., Dugast-Darzacq, C. et al. (2014) Single-molecule tracking in live cells reveals distinct target-search strategies of transcription factors in the nucleus. *eLife* **3**, e02230 https://doi.org/10.7554/eLife.02230

32 Normanno, D., Boudarène, L., Dugast-Darzacq, C., Chen, J., Richter, C., Proux, F. et al. (2015) Probing the target search of DNA-binding proteins in mammalian cells using TetR as model searcher. *Nat. Commun.* **6**, 7357 https://doi.org/10.1038/ncomms8357

33 Mazza, D., Ganguly, S. and McNally, J.G. (2013) Monitoring dynamic binding of chromatin proteins in vivo by single-molecule tracking. *Methods Mol. Biol.* **1042**, 117–137 https://doi.org/10.1007/978-1-62703-526-2_9

34 Harwardt, M.I.E. Dietz, M.S., Heilemann, M. and Wohland, T. (2018) SPT and imaging FCS provide complementary information on the dynamics of plasma membrane molecules. *Biophys. J.* **114**, 2432–2443 https://doi.org/10.1016/j.bpj.2018.03.013

35 Declerck, N. and Royer, C.A. (2013) Interactions in gene expression networks studied by two-photon fluorescence fluctuation spectroscopy. *Methods Enzymol.* **519**, 203–230 https://doi.org/10.1016/B978-0-12-405539-1.00007-5

36 Digman, M.A. and Gratton, E. (2011) Lessons in fluctuation correlation spectroscopy. *Annu. Rev. Phys. Chem.* **62**, 645–668 https://doi.org/10.1146/annurev-physchem-032210-103424

37 Hinde, E. and Cardarelli, F. (2011) Measuring the flow of molecules in cells. *Biophys. Rev.* **3**, 119 https://doi.org/10.1007/s12551-011-0051-x

38 Singh, A.P., Galland, R., Finch-Edmondson, M.L., Grenci, G., Sibarita, J.-B., Studer, V. et al. (2017) 3D protein dynamics in the cell nucleus. *Biophys. J.* **112**, 133–142 https://doi.org/10.1016/j.bpj.2016.11.3196

39 Stortz, M., Angiolini, J., Mocskos, E., Wolosiuk, A., Pecci, A. and Levi, V. (2018) Mapping the dynamical organization of the cell nucleus through fluorescence correlation spectroscopy. *Methods* **140-141**, 10–22 https://doi.org/10.1016/j.ymeth.2017.12.008

40 Mazza, D., Stasevich, T.J., Karpova, T.S. and McNally, J.G. (2012) Monitoring dynamic binding of chromatin proteins in vivo by fluorescence correlation spectroscopy and temporal image correlation spectroscopy. *Methods Mol. Biol.* **833**, 177–200 https://doi.org/10.1007/978-1-61779-477-3_12

41 Liu, Z. and Tjian, R. (2018) Visualizing transcription factor dynamics in living cells. *J. Cell Biol.* **217**, 1181–1191 https://doi.org/10.1083/jcb.201710038

42 Magde, D., Elson, E.L. and Webb, W.W. (1974) Fluorescence correlation spectroscopy. II. An experimental realization. *Biopolymers* **13**, 29–61 https://doi.org/10.1002/bip.1974.360130103

43 Magde, D., Elson, E. and Webb, W.W. (1972) Thermodynamic fluctuations in a reacting system — measurement by fluorescence correlation spectroscopy. *Phys. Rev. Lett.* **29**, 705–708 https://doi.org/10.1103/PhysRevLett.29.705

44 Palmer, A.G. and Thompson, N.L. (1987) Molecular aggregation characterized by high order autocorrelation in fluorescence correlation spectroscopy. *Biophys. J.* **52**, 257–270 https://doi.org/10.1016/S0006-3495(87)83213-7

45 Qian, H. and Elson, E.L. (1990) Distribution of molecular aggregation by analysis of fluctuation moments. *Proc. Natl Acad. Sci. U.S.A.* **87**, 5479–5483 https://doi.org/10.1073/pnas.87.14.5479

46 Qian, H. and Elson, E.L. (1990) On the analysis of high order moments of fluorescence fluctuations. *Biophys. J.* **57**, 375–380 https://doi.org/10.1016/S0006-3495(90)82539-X

47 Chen, Y., Muller, J.D., So, P.T. and Gratton, E. (1999) The photon counting histogram in fluorescence fluctuation spectroscopy. *Biophys. J.* **77**, 553–567 https://doi.org/10.1016/S0006-3495(99)76912-2

48 Aguilar-Arnal, L., Ranjit, S., Stringari, C., Orozco-Solis, R., Gratton, E. and Sassone-Corsi, P. (2016) Spatial dynamics of SIRT1 and the subnuclear distribution of NADH species. *Proc. Natl Acad Sci. U.S.A.* **113**, 12715–12720 https://doi.org/10.1073/pnas.1609227113

49 Clark, N.M., Hinde, E., Winter, C.M., Fisher, A.P., Crosti, G., Blilou, I. et al. (2016) Tracking transcription factor mobility and interaction in *Arabidopsis* roots with fluorescence correlation spectroscopy. *eLife* **5**, e14770 https://doi.org/10.7554/eLife.14770

50 Gaglia, G. and Lahav, G. (2014) Constant rate of p53 tetramerization in response to DNA damage controls the p53 response. *Mol. Syst. Biol.* **10**, 753 https://doi.org/10.15252/msb.20145168

51 Hinde, E., Pandžić, E., Yang, Z., Ng, I.H.W., Jans, D.A., Bogoyevitch, M.A. et al. (2016) Quantifying the dynamics of the oligomeric transcription factor STAT3 by pair correlation of molecular brightness. *Nat. Commun.* **7**, 11047 https://doi.org/10.1038/ncomms11047

52 Kaur, G., Costa, M.W., Nefzger, C.M., Silva, J., Fierro-González, J.C., Polo, J.M. et al. (2013) Probing transcription factor diffusion dynamics in the living mammalian embryo with photoactivatable fluorescence correlation spectroscopy. *Nat. Commun.* **4**, 1637 https://doi.org/10.1038/ncomms2657

53 Presman, D.M., Ganguly, S., Schiltz, R.L., Johnson, T.A., Karpova, T.S. and Hager, G.L. (2016) DNA binding triggers tetramerization of the glucocorticoid receptor in live cells. *Proc. Natl Acad Sci. U.S.A.* **113**, 8236–8241 https://doi.org/10.1073/pnas.1606774113

54 Hinde, E., Cardarelli, F., Digman, M.A. and Gratton, E. (2012) Changes in chromatin compaction during the cell cycle revealed by micrometer-scale measurement of molecular flow in the nucleus. *Biophys. J.* **102**, 691–697 https://doi.org/10.1016/j.bpj.2011.11.4026

55 Hinde, E., Cardarelli, F., Digman, M.A., Kershner, A., Kimble, J. and Gratton, E. (2011) The impact of mitotic versus interphase chromatin architecture on the molecular flow of EGFP by pair correlation analysis. *Biophys. J.* **100**, 1829–1836 https://doi.org/10.1016/j.bpj.2011.02.024

56 Digman, M.A. and Gratton, E. (2009) Imaging barriers to diffusion by pair correlation functions. *Biophys. J.* **97**, 665–673 https://doi.org/10.1016/j.bpj.2009.04.048

57 Moustaqil, M., Fontaine, F., Overman, J., McCann, A., Bailey, T.L., Rudolffi Soto, P. et al. (2018) Homodimerization regulates an endothelial specific signature of the SOX18 transcription factor. *Nucleic Acids Res.* **46**, 11381–11395 https://doi.org/10.1093/nar/gky897

58 Michelman-Ribeiro, A., Mazza, D., Rosales, T., Stasevich, T.J., Boukari, H., Rishi, V. et al. (2009) Direct measurement of association and dissociation rates of DNA binding in live cells by fluorescence correlation spectroscopy. *Biophys. J.* **97**, 337–346 https://doi.org/10.1016/j.bpj.2009.04.027

59 Chen, J., Zhang, Z., Li, L., Chen, B.-C., Revyakin, A., Hajj, B. et al. (2014) Single-molecule dynamics of enhanceosome assembly in embryonic stem cells. *Cell* **156**, 1274–1285 https://doi.org/10.1016/j.cell.2014.01.062

1127

60   Pernus, A. and Langowski, J. (2015) Imaging Fos-Jun transcription factor mobility and interaction in live cells by single plane illumination-fluorescence cross correlation spectroscopy. *PLoS ONE* **10**, e0123070 https://doi.org/10.1371/journal.pone.0123070

61   Tan, F.H., Putoczki, T., Lou, J., Hinde, E., Hollande, F., Giraud, J. et al. (2018) Ponatinib inhibits multiple signaling pathways involved in STAT3 signaling and attenuates colorectal tumor growth. *Cancers (Basel)* **10**, E526 https://doi.org/10.3390/cancers10120526

62   Cutrale, F., Rodriguez, D., Hortigüela, V., Chiu, C.-L., Otterstrom, J., Mieruszynski, S. et al. (2019) Using enhanced number and brightness to measure protein oligomerization dynamics in live cells. *Nat. Protoc.* **14**, 616–638 https://doi.org/10.1038/s41596-018-0111-9

63   Nolan, R., Iliopoulou, M., Alvarez, L. and Padilla-Parra, S. (2018) Detecting protein aggregation and interaction in live cells: a guide to number and brightness. *Methods* **140-141**, 172–177 https://doi.org/10.1016/j.ymeth.2017.12.001

64   Lanzanò, L., Scipioni, L., Di Bona, M., Bianchini, P., Bizzarri, R., Cardarelli, F. et al. (2017) Measurement of nanoscale three-dimensional diffusion in the interior of living cells by STED-FCS. *Nat. Commun.* **8**, 65 https://doi.org/10.1038/s41467-017-00117-2

65   Sezgin, E., Schneider, F., Galiani, S., Urbančič, I., Waithe, D., Lagerholm, B.C. et al. (2019) Measuring nanoscale diffusion dynamics in cellular membranes with super-resolution STED-FCS. *Nat. Protoc.* **14**, 1054–1083 https://doi.org/10.1038/s41596-019-0127-9

66   Scipioni, L., Lanzano, L., Diaspro, A. and Gratton, E. (2018) Comprehensive correlation analysis for super-resolution dynamic fingerprinting of cellular compartments using the Zeiss Airyscan detector. *Nat. Commun.* **9**, 5120 https://doi.org/10.1038/s41467-018-07513-2

67   Grimm, J.B., Muthusamy, A.K., Liang, Y., Brown, T.A., Lemon, W.C., Patel, R. et al. (2017) A general method to fine-tune fluorophores for live-cell and in vivo imaging. *Nat. Methods* **14**, 987–994 https://doi.org/10.1038/nmeth.4403

68   Chen, Y., Johnson, J., Macdonald, P., Wu, B. and Mueller, J.D. (2010) Observing protein interactions and their stoichiometry in living cells by brightness analysis of fluorescence fluctuation experiments. *Methods Enzymol.* **472**, 345–363 https://doi.org/10.1016/S0076-6879(10)72026-7

69   Macdonald, P., Johnson, J., Smith, E., Chen, Y. and Mueller, J.D. (2013) Brightness analysis. *Methods Enzymol.* **518**, 71–98 https://doi.org/10.1016/B978-0-12-388422-0.00004-2

70   Macdonald, P.J., Johnson, J., Chen, Y. and Mueller, J.D. (2014) Brightness experiments. *Methods Mol. Biol.* **1076**, 699–718 https://doi.org/10.1007/978-1-62703-649-8_32

71   Chen, Y., Wei, L.N. and Muller, J.D. (2003) Probing protein oligomerization in living cells with fluorescence fluctuation spectroscopy. *Proc. Natl Acad. Sci. U.S.A.* **100**, 15492–15497 https://doi.org/10.1073/pnas.2533045100

72   Muller, J.D., Chen, Y. and Gratton, E. (2000) Resolving heterogeneity on the single molecular level with the photon-counting histogram. *Biophys. J.* **78**, 474–486 https://doi.org/10.1016/S0006-3495(00)76610-0

73   Petrasek, Z., Ries, J. and Schwille, P. (2010) Scanning FCS for the characterization of protein dynamics in live cells. *Methods Enzymol.* **472**, 317–343 https://doi.org/10.1016/S0076-6879(10)72005-X

74   Ries, J., Chiantia, S. and Schwille, P. (2009) Accurate determination of membrane dynamics with line-scan FCS. *Biophys. J.* **96**, 1999–2008 https://doi.org/10.1016/j.bpj.2008.12.3888

75   Malacrida, L., Hedde, P.N., Ranjit, S., Cardarelli, F. and Gratton, E. (2018) Visualization of barriers and obstacles to molecular diffusion in live cells by spatial pair-cross-correlation in two dimensions. *Biomed. Opt. Express* **9**, 303–321 https://doi.org/10.1364/BOE.9.000303

76   Dertinger, T., Pacheco, V., von der Hocht, I., Hartmann, R., Gregor, I. and Enderlein, J. (2007) Two-focus fluorescence correlation spectroscopy: a new tool for accurate and absolute diffusion measurements. *Chemphyschem* **8**, 433–443 https://doi.org/10.1002/cphc.200600638

77   Di Rienzo, C., Cardarelli, F., Di Luca, M., Beltram, F. and Gratton, E. (2016) Diffusion tensor analysis by two-dimensional pair correlation of fluorescence fluctuations in cells. *Biophys. J.* **111**, 841–851 https://doi.org/10.1016/j.bpj.2016.07.005

78   Petersen, N.O., Hoddelius, P.L., Wiseman, P.W., Seger, O. and Magnusson, K.E. (1993) Quantitation of membrane receptor distributions by image correlation spectroscopy: concept and application. *Biophys. J.* **65**, 1135–1146 https://doi.org/10.1016/S0006-3495(93)81173-1

79   Wiseman, P.W. (2015) Image correlation spectroscopy: principles and applications. *Cold Spring Harb. Protoc.* **2015**, 336–348 https://doi.org/10.1101/pdb.top086124

80   Wiseman, P.W., Brown, C.M., Webb, D.J., Hebert, B., Johnson, N.L., Squier, J.A. et al. (2004) Spatial mapping of integrin interactions and dynamics during cell migration by image correlation microscopy. *J. Cell Sci.* **117**, 5521–5534 https://doi.org/10.1242/jcs.01416

81   Wiseman, P.W., Hoddelius, P., Petersen, N.O. and Magnusson, K.E. (1997) Aggregation of PDGF-beta receptors in human skin fibroblasts: characterization by image correlation spectroscopy (ICS). *FEBS Lett.* **401**, 43–48 https://doi.org/10.1016/S0014-5793(96)01429-X

82   Ranjit, S., Lanzano, L. and Gratton, E. (2014) Mapping diffusion in a living cell via the phasor approach. *Biophys. J.* **107**, 2775–2785 https://doi.org/10.1016/j.bpj.2014.08.041

83   Digman, M.A. and Gratton, E. (2009) Analysis of diffusion and binding in cells using the RICS approach. *Microsc. Res. Tech.* **72**, 323–332 https://doi.org/10.1002/jemt.20655

84   Digman, M.A., Wiseman, P.W., Horwitz, A.R. and Gratton, E. (2009) Detecting protein complexes in living cells from laser scanning confocal image sequences by the cross correlation raster image spectroscopy method. *Biophys. J.* **96**, 707–716 https://doi.org/10.1016/j.bpj.2008.09.051

85   Scipioni, L., Di Bona, M., Vicidomini, G., Diaspro, A. and Lanzanò, L. (2018) Local raster image correlation spectroscopy generates high-resolution intracellular diffusion maps. *Commun. Biol.* **1**, 10 https://doi.org/10.1038/s42003-017-0010-6

86   Hendrix, J., Dekens, T., Schrimpf, W. and Lamb, D.C. (2016) Arbitrary-region raster image correlation spectroscopy. *Biophys. J.* **111**, 1785–1796 https://doi.org/10.1016/j.bpj.2016.09.012

87   Digman, M.A., Dalal, R., Horwitz, A.F. and Gratton, E. (2008) Mapping the number of molecules and brightness in the laser scanning microscope. *Biophys. J.* **94**, 2320–2332 https://doi.org/10.1529/biophysj.107.114645

88   Digman, M.A., Wiseman, P.W., Choi, C., Horwitz, A.R. and Gratton, E. (2009) Stoichiometry of molecular complexes at adhesions in living cells. *Proc. Natl Acad. Sci. U.S.A.* **106**, 2170–2175 https://doi.org/10.1073/pnas.0806036106

89   Nolan, R., Alvarez, L.A., Griffiths, S.C., Elegheert, J., Siebold, C. and Padilla-Parra, S. (2018) Calibration-free in vitro quantification of protein homo-oligomerization using commercial instrumentation and free, open source brightness analysis software. *J. Vis. Exp.* https://doi.org/10.3791/58157

90   Hebert, B., Costantino, S. and Wiseman, P.W. (2005) Spatiotemporal image correlation spectroscopy (STICS) theory, verification, and application to protein velocity mapping in living CHO cells. *Biophys. J.* **88**, 3601–3614 https://doi.org/10.1529/biophysj.104.054874

91   Kolin, D.L. and Wiseman, P.W. (2007) Advances in image correlation spectroscopy: measuring number densities, aggregation states, and dynamics of fluorescently labeled macromolecules in cells. *Cell Biochem. Biophys.* **49**, 141–164 https://doi.org/10.1007/s12013-007-9000-5

92   Pandzic, E., Abu-Arish, A., Whan, R.M., Hanrahan, J.W. and Wiseman, P.W. (2018) Velocity landscape correlation resolves multiple flowing protein populations from fluorescence image time series. *Methods* **140-141**, 126–139 https://doi.org/10.1016/j.ymeth.2018.02.011

93   Wiseman, P.W. (2013) Image correlation spectroscopy: mapping correlations in space, time, and reciprocal space. *Methods Enzymol.* **518**, 245–267 https://doi.org/10.1016/B978-0-12-388422-0.00010-8

94   Cardarelli, F. (2018) Spatiotemporal fluctuation analysis of molecular diffusion laws in live-cell membranes. *Methods Mol. Biol.* **1702**, 277–290 https://doi.org/10.1007/978-1-4939-7456-6_13

95   Di Rienzo, C., Gratton, E., Beltram, F. and Cardarelli, F. (2013) Fast spatiotemporal correlation spectroscopy to determine protein lateral diffusion laws in live cell membranes. *Proc. Natl Acad. Sci. U.S.A.* **110**, 12307–12312 https://doi.org/10.1073/pnas.1222097110

96   Di Rienzo, C., Gratton, E., Beltram, F. and Cardarelli, F. (2014) From fast fluorescence imaging to molecular diffusion law on live cell membranes in a commercial microscope. *J. Vis. Exp.*, e51994 https://doi.org/10.3791/51994

97   Di Rienzo, C., Piazza, V., Gratton, E., Beltram, F. and Cardarelli, F. (2014) Probing short-range protein Brownian motion in the cytoplasm of living cells. *Nat. Commun.* **5**, 5891 https://doi.org/10.1038/ncomms6891